



INSTITUT DE FRANCE
Académie des sciences

Comptes Rendus

Mécanique

Kaili Xie and Marc Leonetti

Mechanical characterization of core-shell microcapsules


Volume 351, Special Issue S2 (2023), p. 163-182

Published online: 6 April 2023

<https://doi.org/10.5802/crmeca.148>

Part of Special Issue: Physical Science in Microgravity within the Thematic Group
Fundamental and Applied Microgravity

Guest editors: Olga Budenkova (CNRS, Université Grenoble Alpes, Grenoble INP, SIMaP, 38000 Grenoble, France), Catherine Colin (IMFT, Université de Toulouse, CNRS, INPT, UPS et GDR 2799 Micropesanteur Fondamentale et Appliquée) and Guillaume Legros (ICARE, CNRS UPR 3021, Univ. Orléans et GDR 2799 Micropesanteur Fondamentale et Appliquée)

 This article is licensed under the
CREATIVE COMMONS ATTRIBUTION 4.0 INTERNATIONAL LICENSE.
<http://creativecommons.org/licenses/by/4.0/>



*Les Comptes Rendus. Mécanique sont membres du
Centre Mersenne pour l'édition scientifique ouverte*

www.centre-mersenne.org

e-ISSN : 1873-7234



Physical Science in Microgravity within the Thematic Group Fundamental and Applied Microgravity / *Sciences physiques en microgravité au sein du GDR Micropesanteur Fondamentale et Appliquée*

Mechanical characterization of core-shell microcapsules

Kaili Xie[Ⓢ] ^a and Marc Leonetti[Ⓢ] ^{*, b}

^a Univ. Bordeaux, CNRS, LOMA, UMR 5798, F-33400 Talence, France

^b Aix Marseille Univ, CNRS, CINaM, Marseille, France

E-mails: kaili.xie@u-bordeaux.fr (K.Xie), marc.leonetti@univ-amu.fr (M. Leonetti)

Abstract. Core-shell configurations are ubiquitous in nature such as in the form of bacterial and cells. Inspired by this, microcapsules are designed with actives as the cores surrounded by thin shells. They not only play an increasing role as artificial models for understanding dynamic behaviors of biological cells in flows, but are also becoming a fundamental class of artificial vehicles at the heart of drug delivery and release in applications. The mechanical properties of the shells are of great importance in this context. Here, we review recent experimental and theoretical characterizations of microcapsules, focusing on the soft and deformable particles with liquid cores. We begin by exploring the concept and fabrication of artificial microcapsules, followed by a discussion of different methods on the mechanical characterization of the shell.

Keywords. capsule, vesicle, RBC, interfaces, interfacial rheology, encapsulation, polymers.

Published online: 6 April 2023

1. Introduction

In nature, core-shell particles are commonly found in various forms such as bacteria and cells [1], with scales ranging from a few nanometers up to several millimeters (Figure 1). The shell encloses and protects the core material from the surrounding environment, while also mediates core-environment interactions through well defined and controllable pathways for the substance transfer and exchange. Recently, synthetic microcapsules have attracted increasing attention in food, cosmetics, and biomedicine applications [2–4]. Research has primarily focused on encapsulation techniques, development of shell materials, and assembly strategies for different purposes [5–8]. One of the most promising use of synthetic microcapsules is the delivery of drugs under controllable release [9]. Actives can be loaded into the microcapsules and then transferred to the target sites. External stimuli, such as pH values [10], temperatures [11], or stresses [12–14] are often considered as the effective strategies to release the contents through permeability changes or mechanical degradation of the shell. The design of functional microcapsules for

* Corresponding author.

specific purposes requires the well-controlled and known shell properties such as the structure and mechanical properties.

The determination of the shell mechanical properties is essential for investigating the stability of microcapsules against the external forces, e.g., shear and stretch. A sufficiently robust shell is required when the microcapsules are used as microscale reactors [15]. For example, the encapsulated catalysts or enzymes have to be protected from degradation, and retained within the microcapsules during mixing. The shell rupture in contrast may be desired as a pathway for efficient and rapid release of the core materials when the microcapsules flow and deform in the fluid medium [14, 16]. The tuning of the shell properties is correlated to the preparation process of the microcapsules [6, 17].

There are various techniques to probe the mechanical properties of the shell of microcapsules. This review aims to summarize the principles behind these approaches as well as the conditions of their utilization. In what follows, we begin the concept of microcapsules and their shell deformation. Following this, we cover different methods for the determination of the shell properties, for a single microcapsule, from both the local and global deformations. In this review, we intend to provide a summary of the most recent developments on liquid-core microcapsule characterizations which are accessible in laboratory measurements. An in-depth analysis is beyond the scope of this review article.

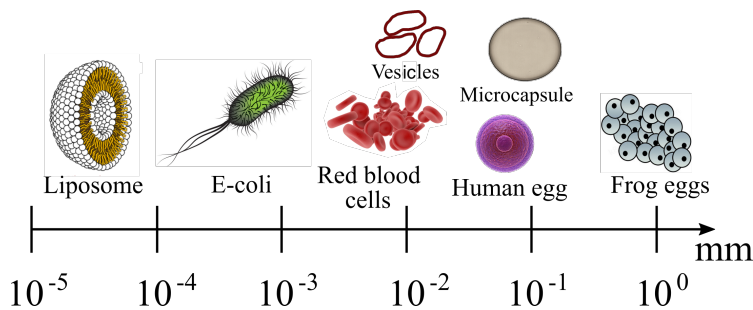


Figure 1. Scale overview of various core-shell configurations in nature (adapted from Ref. [18]).

2. Microcapsules: concept and shell assembly

A wide range of capsule systems has been developed and investigated for various aims in different communities. There is probably no clear boundary among them regarding the definition. However, it is generally accepted that a microcapsule has a core material which is surrounded or coated with a continuous shell [19]. The core-shell configuration is hence the primary nature of microcapsules. Depending on the purposes, the core materials can be liquid, solid, and even gas (hollow microcapsules). In most cases, the shell is solid and it generally has a thickness much smaller than the dimension of the microcapsule. The formation of the shell can be achieved by cross-linking or physical bonding [2]. The process of preparing the microcapsules is called encapsulation. In this review, we limit our focus on the deformable microcapsules with a liquid content and a thin elastic or viscoelastic shell. This type of microcapsules is often considered as a simple physical model for understanding the dynamic behaviours of biological cells, for example Red Blood Cells (RBCs) in the blood circulation [20–23].

Microcapsules tend to be confused with other deformable particles, such as RBCs [24], polymeric vesicles [25], and vesicles [26] due to their resemblance [27]. We here briefly clarify their differences in terms of the shell structure and mechanical properties. Vesicles have a membrane that

consists of a lipid bilayer. RBCs have a spectrin network beneath a lipid bilayer with anchored membrane proteins. This shell also called membrane has a shear resistance [28] (Figure 2a, b). The lipid bilayers are incompressible, and thus the membrane surface area is often considered as constant in deformation [29–31] even in the case of large deformation [32, 33]. The membrane is more likely to bend rather than to be compressed or stretched [34]. Note that the lipid bilayers in the membrane of vesicles is fluid and the two monolayers can slide over each other. The physical properties of polymersomes are close to lipid layers but with a high two-dimensional shear viscosity. A striking difference between vesicles and capsules is the emergence of vortices at the membrane of vesicles [35, 36]. Associated to this material property, microcapsules have a reference state different from vesicles.

The composite capsule shell (Figure 2c) has elastic and viscous resistances against the shear and dilation deformations. The deformation occurs through stretching the shell at the cost of elastic energy. The bending resistance is often neglected when studying the overall deformation of microcapsules. However, it does play an important role in the local modulation of the shape such as wrinkling or folding as evoked previously [18, 37]. Conveniently, the mechanical properties of microcapsules can be tunable by controlling the polymerization process which can be handled precisely using microfluidics [6].

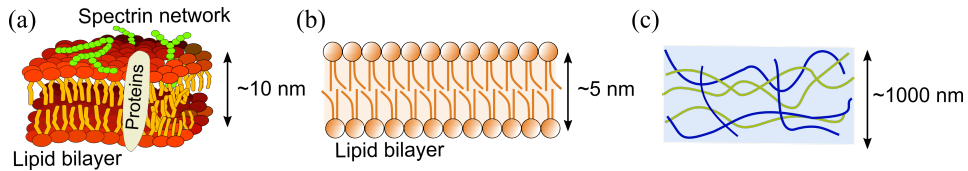


Figure 2. Illustration of the membrane/shell structures of (a) red blood cells, (b) vesicles, and (c) microcapsules.

There are various well developed methods for assembling the shell of microcapsules [2]. However, if we limit ourselves to the microcapsules with fluid cores wrapped by elastic shells, the assembly process can, in general, be classified into two categories: polymerization/cross-linking [38] and interaction bonding [39, 40]. Two steps are generally involved: the formation of droplets by emulsification, and the shell assembly at the droplets interfaces. By stirring the emulsion the monomers migrate to the water/oil interface and polymerize. The droplets are stabilized avoiding coalescence for example. The degree of interface polymerization significantly affects the shell mechanical properties. Typical examples are nylon capsules [41], polysiloxane microcapsules [42], and albumin microcapsules [17]. If oppositely charged polyelectrolytes exist in the immiscible phases, the shell can be formed by interaction bonding such as electrostatic adsorption [6, 7] and H-bonding [5, 40]. The layer-by-layer (LbL) technique is introduced to precisely tailor the structure and mechanical properties of the shell of the microcapsules. Additional details on this subject can be found in recent review paper [2].

3. Shell deformation of microcapsules

From the mechanical point of view, it is more interesting to understand how the shell of a microcapsule undergoes deformation. Indeed, the deformability of the shell closely depends on the assembly process during the microcapsule fabrication. Regarding the mechanical behaviours, several constitutive laws had been proposed in the past decades [1]. The proper constitutive law for a certain type of capsules could be chosen by a combination of experimental and numerical investigations [43].

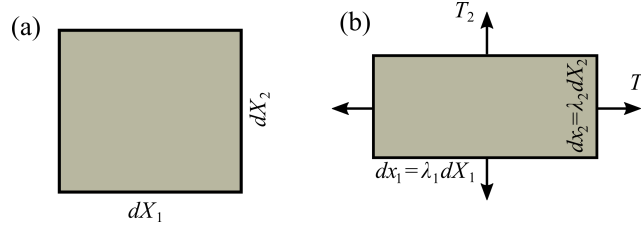


Figure 3. An element of 2D membrane in deformation. (a) Reference shape. (b) Deformed shape with extension ratios λ_1 and λ_2 under the principal tensions T_1 and T_2 .

As mentioned above, the thickness of the shell is much smaller than the capsule size, typically smaller than 10% of the capsule radius. The transverse shear stress vanishes across the thickness of the shell allowing the use of a two-dimensional elasticity framework. The bending resistance is often neglected [1, 44], but essential if surface wrinkling or buckling instabilities appear [18, 37]. The shell can thus be treated as a two-dimensional membrane (Figure 3 and Figure 4), associated to the constitutive laws or the laws of behaviours. In this framework, when stretched or compressed, the membrane only undergoes in-plane deformation. The tension tensor \mathbf{T} can be decomposed into two principal directions associated to two eigenvalues T_1 and T_2 (Figure 3). The deformation is simply related with two principal extension ratios by $dx_1 = \lambda_1 dX_1$, $dx_2 = \lambda_2 dX_2$. Constitutive laws give the stress-strain relationship [43, 45, 46] beginning by the most classic one, the generalized Hooke model:

$$T_1^{GH} = \frac{G_s}{1 - \nu_s} \frac{\lambda_1}{\lambda_2} [\lambda_1^2 - 1 + \nu_s (\lambda_2^2 - 1)], \quad (1)$$

where ν_s is the surface Poisson's ratio, G_s the surface shear elastic modulus. The unit is the N/m or Pa·m. Indeed, $G_s = Gh = Eh/2(1 + \nu_s)$, where G , h , and E are the bulk shear modulus, the thickness, and the bulk Young modulus (Pa), respectively. In order to recall that the non-linearities are preserved in the strain-stress tensor, the term *generalized* is preferred to distinguish from the linearized Hooke model:

$$T_1^H = \frac{G_s}{1 - \nu_s} [\lambda_1^2 - 1 + \nu_s (\lambda_2^2 - 1)]. \quad (2)$$

The corresponding expressions for T_2 can be obtained by interchanging the roles of indices 1 and 2 in the following equations. In the limit of small deformations (linear regime), all the elastic models reduce to the Hooke model.

If the membrane material exhibits a strain-softening property, e.g., rubber-like or gelled material, a neo-Hookean law (NH) is given by

$$T_1^{NH} = \frac{G_s}{\lambda_1 \lambda_2} \left[\lambda_1^2 - \frac{1}{\lambda_1^2 \lambda_2^2} \right]. \quad (3)$$

The NH law can be used to model the behaviour of an infinitely thin membrane that is volume incompressible and isotropic, but it may not work well to model the area-incompressible membrane [1]. A general expression of NH law is referred to as the Mooney–Rivlin (MR) law,

$$T_1^{MR} = \frac{G_s}{\lambda_1 \lambda_2} \left(\lambda_1^2 - \frac{1}{\lambda_1^2 \lambda_2^2} \right) [\Psi + \lambda_2^2 (1 - \Psi)], \quad (4)$$

where Ψ is a coefficient ranging between 0 and 1. When $\Psi = 1$, it reduces to the NH law. The use of Ψ intends to compensate the area dilation by the corresponding thinning of the membrane in deformation.

Another law often used to model the strain-hardening material, such as RBCs membrane, is proposed by R. Skalak et al. [47],

$$T_1^{SK} = \frac{G_s}{\lambda_1 \lambda_2} [\lambda_1^2 (\lambda_1^2 - 1) + C \lambda_1^2 \lambda_2^2 (\lambda_1^2 \lambda_2^2 - 1)], \quad (5)$$

where $C = v_s / (1 - v_s)$ is the tuning parameter concerning the membrane area incompressibility. For example, the RBC membrane has a lipid bilayer which is almost area incompressible but easy to shear. In this case, the coefficient should be $C \gg 1$. However, in simulation, C is often equal to 1 or 10 due to numerical constraints with sometimes a global penalization of the area. Also, as for all elastic models, the membrane fluidity of RBCs is lost.

These elastic laws will show differences in the membrane behaviour as soon as it undergoes moderate deformation. Detailed comparisons can be found in the references [19, 43, 44, 46]. The investigation of the overall deformed shape and the dynamics (stationary shape, oscillations, and tumbling, etc.) has been largely performed by neglecting the bending energy. In fact, these motions lead to deformations that exhibit an order of magnitude of the particle size. The bending tension scales as B/R^2 , while the in-plane elastic tension scales as G_s , where $B = Eh^3/[12(1 - \nu_s^2)]$ is the bending modulus and R is the capsule radius. The ratio of these tensions is proportional to $(h/R)^2 \ll 1$; typically, $h \approx 100$ nm and $R \approx 50$ μ m for a capsule made of chitosan for example. The bending energy has to be taken into account when the local patterns, such as wrinkles or folds, appear [48].

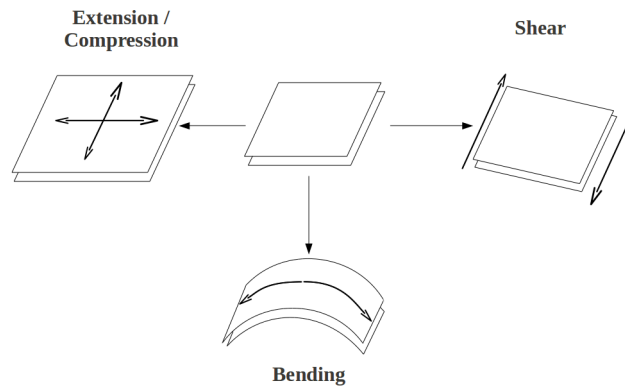


Figure 4. The microcapsule shell deformations: dilation, shear and bending resistances.

4. Mechanical characterization

The determination of the mechanical properties of individual capsules is interesting to represent the diversity of shell properties, and further to point a guide to optimize the synthetic process. In this section, we summarize the characterization methods which have been validated for liquid-core capsules, including plate-plate compression, local indentation, aspiration, and flow-induced deformation.

4.1. Compression

A straightforward way to deform a spherical capsule is to apply forces on the capsule by compression [49, 50] (see Figure 5). This can be achieved by using two parallel planes in which the forces

and moving distance are simultaneously measured. Such technique can be traced back to as early as 1932 when Cole studied the surface forces of sea urchin eggs [51]. Later, well controlled plate-plate compression systems have been established: see notably the works of the group of Zhibing Zhang [52]. The capsule can be compressed at a speed as low as a few micrometers per second with a force range from μN to N . Smaller capsule (in microscale) is also accessible to be compressed. Imaging with the high resolution camera allows to detect the quasi-static profile of the deformed capsule. Multiple views make it possible to understand the origin of shell bursting during compression [53].

In experiments, the measuring force monotonically increases with the compression [53, 54]. For small deformation (approximately below 5% deformation), the Reissner model [55] illustrates the linear force-displacement relationship for a hollow capsule under compression. Lytra et al. [56] recently extended the Reissner model for capsule deformation up to 50%,

$$F = \frac{4Eh^2}{\sqrt{3(1-\nu^2)}} \frac{\delta}{a} + \pi \frac{4Eh}{a^2} \delta^3 \quad (6)$$

where h is the shell thickness, a is the radius of undeformed capsules, δ is half the value of the distance change between the two plates. There are only two unknown parameters: the Young's modulus E (unit: Pa) and the Poisson's ratio ν of the shell. Generally, for polymeric capsule ν is supposed to be close to 0.5 for the sake of simplicity (see further). By fitting the experimental data using Equation (6), the elastic modulus can be measured reliably even for a liquid-core capsule [57]. For gellan gum microcapsules, this technique yields to measure the shell Young's modulus ranging from 10 kPa to 50 kPa, depending on the concentration of gellan gum [57].

However, for large deformation a more sophisticated mechanical analysis has to be conducted. Its derivation was originally performed by Feng and Yang [58]. Properties such as the shear modulus and the dilation modulus can then be determined by combining the experimental and numerical results [19, 53]. Capsules prepared by crosslinking human serum albumin (HSA) with alginate [53] are found to have a surface shear modulus of $G_s = 4.4 \text{ N/m}$ for a thickness of $68 \mu\text{m}$ and $G_s = 1.6 \text{ N/m}$ for a thickness of $30 \mu\text{m}$. If the Poisson's ratio is assumed to be 0.5, the Young's modulus is obtained around $E = 3G_s/h = 0.18 \pm 0.02 \text{ MPa}$.

Since liquid-core capsules are often immersed into another fluid, it is worth to note that low squeezing speed is preferred during compression to ensure that the equilibrium state is achieved, and to avoid flow effect in each step. Nevertheless, the constant application of the force, particularly for longer periods of time, will induce mass exchange between the interior and exterior of the capsule, and further change the deformation response. Therefore, the osmotic change has to be avoided by careful preparation of the microcapsules and choice of compression speed. Another limit of the plate-plate compression method is that it may not be applicable for small shell thickness (e.g., $h < 1 \mu\text{m}$) of capsules as they tend to break during compression even for small deformation.

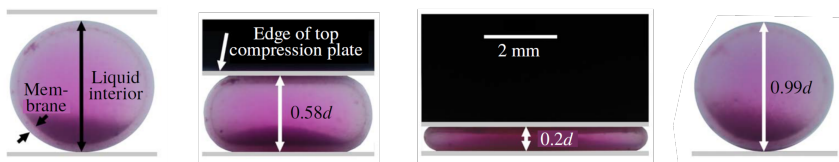


Figure 5. Side-view images of a capsule under the axial compression in a saline solution. After removing the top plate, the capsule has returned to its undeformed shape. Adapted from Ref. [54].

4.2. Indentation

Another technique similar to the plate-plate compression is deforming microcapsule by the use of an atomic force microscope (AFM). Differently, AFM indentation can apply a smaller force ranging from pN to μN , which makes it possible to manipulate on much softer microcapsules [59]. AFM has been established in various measurements such as topography, adhesion [60], and interface rheology [61]. One of the advantages of AFM is that it can directly measure the deformation (indentation displacement) and the force response with high resolution. A typical measurement procedure can be summarized as: 1) selection of a cantilever with suitable stiffness and tip size; 2) cantilever calibration; 3) approaching the tip towards the capsule and measuring the curve of force *versus* displacement; 4) analysis of the force-indentation curve with the appropriate model.

Regarding the capsule size and AFM tip type, there are two typical measurement strategies: colloidal probe (Figure 6a) and sharp probe (Figure 6b). Both methods can induce from a small to large deformation of the capsule shell. However, here we only summarize the small deformation region from which we can extract the mechanical properties of the capsule shell. The indentation is much smaller than the capsule initial size.

A simple measurement was performed by Dubreuil et al. [62] using a home-made colloidal probe on multi-layer polyelectrolyte microcapsules. The force was observed to increase linearly with the indentation up to 100 nm (Figure 7). The loading speed of the AFM tip seems to have no effect on the force-displacement curve at least up to the speed of 200 nm/s. In the linear regime, the deformation of the capsule is reversible for several loading and unloading cycles. The slope of the linear curve, k , can be linked to the capsule shell property, i.e. Young's modulus E by

$$k = \xi \frac{Eh^2}{a} \quad (7)$$

where h is the shell thickness, a is radius of the capsule, and ξ is a coefficient that depends on the Poisson's ratio ν , presenting the form $\xi = 1/[(1+\nu)\sqrt{6(1-\nu)}]$ for pure shear deformation; and $\xi = 1/[(1-\nu)\sqrt{6(1+\nu)}]$ for pure stretch deformation. The shear deformation may occur for the capsules assembled using the layer-by-layer (LbL) method due to sliding between adjacent layers in deformation. However, in most cases both shear and stretch deformations are likely to happen, and it is difficult to distinguish one from the other. If the Poisson's ration is taken as $\nu = 0.5$, the coefficient ξ then ranges between 0.38 and 0.67, which is within the same order of magnitude.

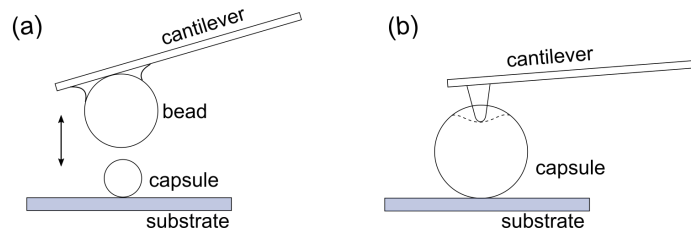


Figure 6. Schematic of indentation on the microcapsule performed by using atomic force microscope. (a) The capsule has a dimension smaller or similar to that of the colloidal on the probe. The different sizes of the beads can be glued onto the cantilever. (b) The AFM tip is much smaller than the capsule dimension.

As mentioned above, the value of the Poisson's ratio ν is generally unknown except the case of albumin capsules where the value 0.4 was determined [43]. However with a close kind of capsules $\nu = 0.5$ was also proposed using a different technique proving that it is still a challenge [63]. Note that some polymer gels such as polyacrylamide have a smaller Poisson's ratio much closer

to $\nu = 0.3$ [64, 65]. Finally, some caution is needed when considering the value of the Poisson's ratio even for cases in which we only wish to determine an approximate order of magnitude of the Young's modulus. Extracting the slope of the force-displacement curve gives the Young's modulus of the capsule shell (Equation (7)). As the indentation is small in the case of colloidal probe measurement, this method is similar to the plate-plate compression in the region of small deformation; Equation (7) has a reduced-order form of the Reissner model (without the second term on the right side of Equation (6)) [66, 67]. In literature, using this method, it is found that the sodium poly(styrene sulfonate)/poly(allylamine hydrochloride) (PSS/PAH) capsules have a value of Young's modulus in a range of 1.5-1.8 GPa [62].

The second measurement method is using a sharp AFM tip which has an effective radius much smaller than the capsule size. The indentation depth is generally only 1~2% of the microcapsule dimension. Thus, it can be approximated to the case of a probe deforming a flat membrane. The Hertz model, taking into account the geometries of the object and the AFM tip, describes the relationship between the force and deformation,

$$F = \frac{4E}{3(1-\nu^2)} \sqrt{a^*} \Delta^{3/2} \quad (8)$$

where $1/a^* = 1/a_t + 1/a_s$, and a_t and a_s are the radius of the AFM tip and capsule, respectively. Δ is the indentation depth. An elastico-adhesion model, Johnson-Kendal-Roberts (JKR) model [68], can be used to better describe the force curves for the cases where adhesion between the AFM tip and the sample is significant. A crucial point of using the sharp AFM tip measurement is to ensure the local deformation of the shell, avoiding the overall nonlinear capsule deformation.

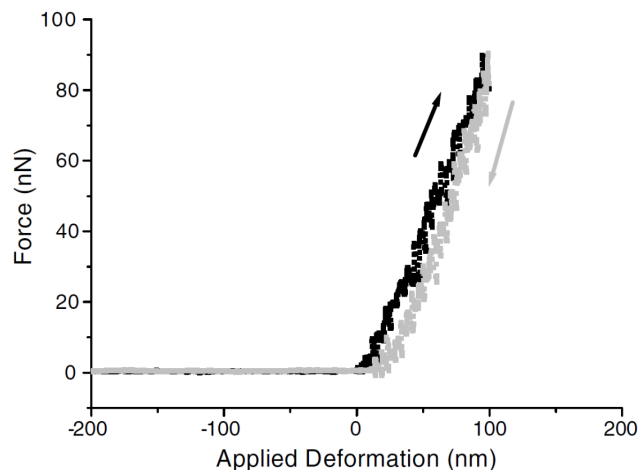


Figure 7. Force-displacement curve in the small-deformation regime for a PSS/PAH capsule [62]. The black curve corresponds to the loading process while the gray one is the unloading process.

The AFM technique is usually limited to thin microcapsule shells. The stiffness selection of the AFM tip is essential to have a high sensitivity. Similar to the plate-plate compression, AFM measurements are often performed in a liquid environment in which the movement of capsule, such as sliding, should be prevented. The effect of dynamic flow should be reduced as much as possible during manipulation. Measurements using the colloidal probe may be less sensitive to local membrane heterogeneities, as the probe size is comparable to the capsule size, unlike

the case of where sharp probes are used. A more recent work [69] compared the results of Young's modulus measurements by AFM nanoindentation and compression test for melamine-formaldehyde (MF) microcapsules. The obtained data showed that both methods give similar results within the standard deviation.

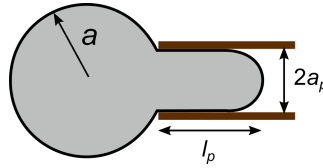


Figure 8. Illustration of micropipette aspiration on a microcapsule. The suction pressure is well controlled by using a precise pressure transducer.

4.3. Micropipette aspiration

Micropipette aspiration is a technique often used to obtain physical properties of biological cells as well as artificial capsules. A micropipette or capillary with a few micrometers in diameter is used to aspirate an elastic capsule with controlled pressure ΔP . A portion of the capsule shell goes into the micropipette with a aspiration length l_p (see Figure 8). The shell is assumed to be homogeneous and incompressible, with a elastic Young's modulus E . In the elastic regime, the shape of the deformed capsule can be linked with the shell mechanical properties by [70, 71]

$$\Delta P = \alpha E \frac{l_p}{a_p}, \quad (9)$$

where a_p is the radius of the micropipette, α is the coefficient related to the sizes of capsule and micropipette, and is given by $\alpha = \beta_1 [1 - (a_p/a)^{\beta_3}] / 3$. The constants $\beta_1 = 2.01$ and $\beta_3 = 2.12$ were obtained numerically by Zhou et al. [72]. A course estimation of the coefficient can also be taken, $\alpha \approx 1$ [73]. The bending rigidity and the stretching elasticity can be deduced with a sophisticated model developed by Henriksen & Ipsen [74].

The pressure control is essential in this aspiration technique. A precise pressure transducer, e.g. microfluidic pump, is preferred but it is usually costly. Hydrostatic pressure offers a simple and low-cost way to adjust the suction pressure by changing the relative height between the micropipette head and the reservoir [71].

A close configuration is the *pendant* capsule, a technique called elastometry [37, 75]. A pendant drop is put at the end of a capillary embedded in an immiscible solvent. The chemical reaction between reactants in both phases takes place at the interface. When the stationary state is reached, a small suction is applied to change the shape slightly. wrinkles appear in the part of the membrane under compression. The measurement of the wavelength is a mean to evaluate the bending modulus independently.

4.4. Characterization by non local stress: hydrodynamic flow

The hydrodynamic flows provide conceptually different approaches to deform microcapsules. The flow strength is tunable by using different viscosities of the external liquids and the flow rates, i.e., shear rate and extensional rate. This approach can be performed in the linear and nonlinear regimes of deformations. The first one allows the determination of elastic moduli using analytical developments. Thanks to accurate numerical codes [76–81], the nonlinear regime allows to fit the

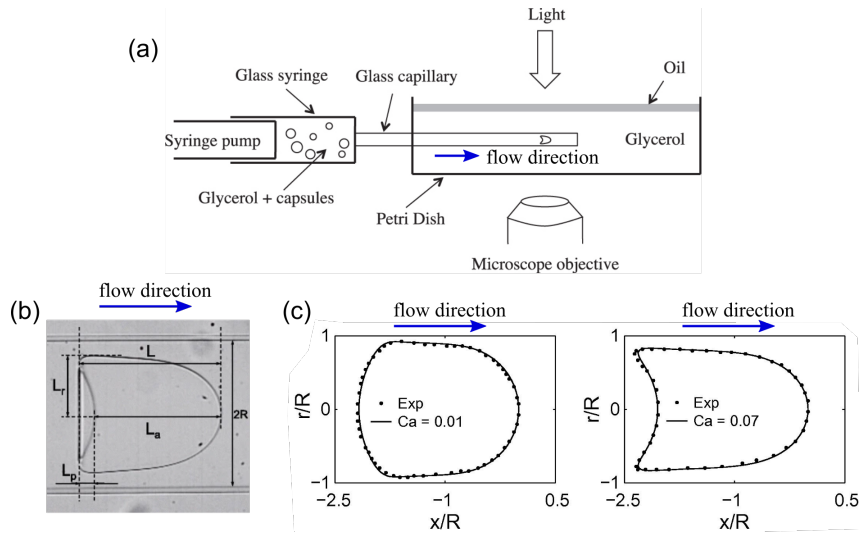


Figure 9. Microcapsules characterization in the confined flow. (a) Schematic of the experimental setup (from Ref. [88]). (b) The profile of a deformed microcapsule in the capillary flow (from Ref. [89]). L , L_a , L_p and L_r are the geometric parameters which can be extracted from the image. R is the radius of the channel. (c) Comparison of the experimental (dotted line) and numerical (continuous line) profiles (from Ref. [63]).

experimental curves to deduce the elastic moduli in a large range of deformations, and it also can help to determine the constitutive law of the membrane material. One advantage of flow is its ability to perform the measurements automatically in batch [63, 82], prefiguring applications on a production line and live analysis. Another advantage is its ability to explore the nonlinear regime and to provide new insights on the constitutive laws. However, as the capsule is free, the role of a mismatch between internal and external densities due to the fabrication or the required application becomes important. Using microgravity is an efficient tool to separate the contributions of gravity from flow. Here, we discuss the main and easily accessible approaches which can be achieved by microfluidic techniques [83, 84].

For a liquid-core capsule deformed in an external viscous flow, the jump of viscous traction across the shell is the driving force that deforms the capsule, and is equal to the load on the shell [1]. The shape of the capsule thus results from the mechanical equilibrium at the interface (a coupling relation) associating the hydrodynamic stresses and the tensions in the shell (Figure 10c).

In experiments, the external viscosity is generally high which leads to a Reynolds number Re that is much smaller than 1: $Re = \rho U a / \eta$, where ρ is the external fluid density, U the typical velocity, η the external fluid viscosity, and a the radius of the capsule. With $\rho \approx 10^3 \text{ kg/m}^3$, $U \approx 1 \text{ mm/s}$, $a \approx 100 \mu\text{m}$ and $\eta \approx 100 \text{ mPa}\cdot\text{s}$, we can obtain $Re \approx 10^{-3}$. Thus, experiments are often performed in the Stokes regime where the theory has been well established [85, 86]. Thanks to the boundary integral method [87], accurate numerical models have been developed. In the regime of small deformation, all the surface elastic models are equivalent. Otherwise, the deformation is closely related to the constitutive laws of the shell material. This is a challenge that can only be solved by numerical investigations.

4.4.1. Confined flow

The confined flow, also called channel flow, is usually achieved by injecting the diluted microcapsules suspension through a small size channel [63, 88–90] (see Figure 9). The cross section of the channel can be round, square, or rectangular. The static shape of the capsule in the confined flow is associated with the size ratio of the capsule to the channel and the flow strength. If the microcapsule has a dimension smaller than the channel size, its shape is only slightly deformed. However, if the size of the microcapsule is comparable to the size of the channel, or even bigger, the shape becomes bullet-like or parachute-like depending on the flow rate (Figure 9c).

The mechanical properties of the microcapsule are obtained by using an inverse analysis method, a technique developed by the BMBI group [63, 91, 92]. The basic idea is to compare the profiles of deformed capsules from the numerical model and the experimental measurement. The initial shape of the microcapsule is assumed to be spherical with a radius a . When it is deformed in the channel, the geometric parameters L , L_a , L_p , and L_r can be measured using image processing, where $L_p = L - L_a$. The confinement ratio is defined as the size of the capsule to the dimension of the channel, a/R . The velocity of the capsule, v , is experimentally measured by a video recording. In the numerical calculation, a constitutive law is selected to model the deformation of the microcapsules in the confined flow. At steady state, the velocity and the shape of the deformed capsule only depend on the confinement ratio a/R and capillary number $Ca = \eta U/G_s$, where η is the viscosity of the external fluid, U is the mean unperturbed velocity of the external liquid, and G_s is the surface shear modulus of the capsule shell.

From the numerical calculation, a database is first created, containing the geometric characteristics L/a , L_a/a , L_r/a and the velocity ratio v/U as function of a/R and Ca . In experiments, the confinement ratio value a/R and the geometric lengths L/a , L_a/a and L_r/a are measurable. By comparing the confinement ratio and geometric lengths from the numerical and the experimental results (where the shape should be very similar within a tolerance), then the Ca and v/U can be known from the database. The shear elastic modulus is given by,

$$G_s = \frac{\eta U}{Ca}. \quad (10)$$

More detailed procedures are recommended to read the references [63, 88, 89, 91]

This method has the capability to measure the mechanical properties of capsules in a high throughput with the advantage of being easily performed using a microfluidic chip. However, the appropriate elastic model to describe the capsule shell deformation has to be chosen primarily. For some types of capsules, the shell materials are complex and the constitutive law is unknown. Experimental and numerical work for determining the shell model have to be done before using this method [43].

4.4.2. Shear flow

Shear flow is another approach to deform the microcapsule. A high aspect ratio channel or the Couette device are often used to generate the shear flow field (see Figure 10a,b). The hydrodynamic stresses are created by the established flow fields of the interior and exterior of the capsule. The steady-state deformation of the capsule is defined as $D_\infty = (L - S)/(L + S)$, where L and S are semi-major and semi-minor axis lengths of the deformed capsule, respectively. In the small deformation regime, an asymptotic solution has been proposed by D. Barthès-Biesel and co-authors [1, 44],

$$D_\infty = \frac{5}{2(c+1)} \frac{2 + \nu_s}{1 + \nu_s} \frac{\eta \dot{\gamma} a}{G_s} \quad (11)$$

where for the shear flow the constant $c = 1$, ν_s the surface Poisson's ratio, G_s the surface shear elastic modulus, and $\dot{\gamma}$ is the shear rate.

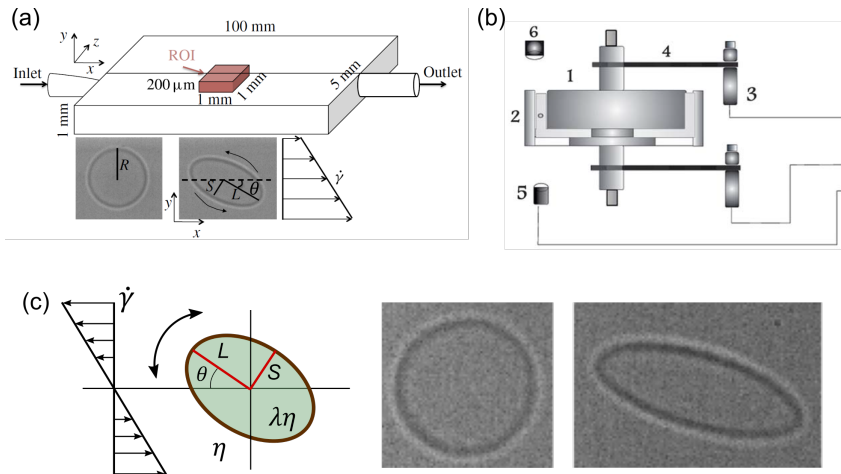


Figure 10. Microcapsule deformation in shear flow. (a) Approximately linear shear flow (ROI) in a high aspect ratio channel (from Ref. [43]). (b) Schematic of the Couette-like rheoscope. 1—inner cylinder, 2—outer cylinder, 3—motor drive unit, 4—belts, 5—microscope objective, 6—light source. (from Ref. [42]). (c) The microcapsule aligned and deformed in the shear flow. The viscosity ratio between the interior and exterior is λ . Images are from Ref. [43].

The steady-state deformation (Equation (11)) of the capsule in shear flow has been verified by various experimental investigations. For instance, H. Rehage and co-authors [42,93,94] measured the rheological properties of polysiloxane microcapsules using a rheoscope setup (Figure 10b). S. Joung et al. [95] used a similar rheoscope to extract the properties of composite microcapsules. de Loubens and co-authors [43,96] have reported that HSA capsules show different mechanical properties depending on the degree of the shell crosslinking. Higher crosslinking gives rise to a larger value of the Young's modulus of the shell.

The measurement here is limited within the small deformation regime (generally $D_\infty \leq 5\%$ for the steady-state deformation). The shear elastic modulus is extracted by plotting the deformation *versus* the shear rate for individual capsules. However, the dynamics of the capsule in shear flow are complex. The deformation may exhibit oscillation due to swinging, tumbling, or tank-treading motions [1, 95, 96]. In practice, it is better to prevent such complex behaviors when measuring the shell mechanical properties.

4.4.3. Extensional flow

The extensional flow is simpler than the shear flow as no tank-treading exists and as the capsule stays at the centre during a sufficient time to reach stationary deformations. The original setup that produces such flow field is the four-roll mill device developed by G. Taylor [97] (Figure 11). The flow field is considered as two-dimensional as no liquid flows vertically, $[v_x, v_y, v_z] = [\dot{\epsilon}x, -\dot{\epsilon}y, 0]$, where $\dot{\epsilon}$ is the extensional rate. The extensional rate can be accurately controlled by changing the rotation speed of the four rolls. At the center of the flow, the velocities $v_x = v_y = v_z = 0$, which is called stagnation point. The field of extensional rate around the stagnation point is roughly constant [6, 17, 82]. To ensure the capsules are exposed to a homogeneous extensional field, they are generally stabilized near the stagnation point in the flow.

Chang & Olbricht [41] are probably the first to use the four-roll mill device to deform synthetic millimetric capsules. The steady-state deformation D_∞ was plotted as a function of various flow

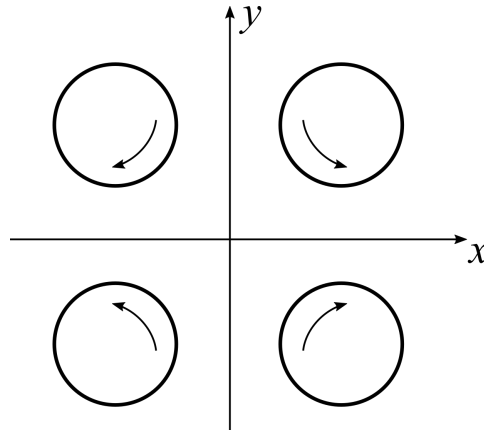


Figure 11. Schematic of the top view of the four-roll mill. The extensional flow field is generated in the center.

strain rates G . It was found that the deformation is linearly related to the strain rate, $D_\infty = 25/2[\eta GR/(Eh)]$, where R is the radius of the capsule, E is the Young's modulus, and h is the thickness of the capsule shell. Fitting the experimental data gives the mechanical property Eh of the shell which is considered as the two-dimensional modulus, i.e. surface Young's modulus. Compared to the plate-plate compression, the values of surface Young's modulus from the extensional flow measurement are slightly higher, but they are within the same order, between 0.1-0.4 N/m for the case of the nylon capsules.

Microfluidics has been recently used to create the extensional flow field to deform capsules [6, 17, 84, 98]. The extensional rate $\dot{\epsilon}$ is easily adjustable by the flow rate. A diluted microcapsules suspension is injected into the extensional flow chip through a syringe. Individual microcapsules pass the stagnation point and deform. The steady-state deformation is achieved by stabilizing the capsule near the stagnation point for a long enough period of time (Figure 12a).

Equation (11) also gives the prediction of capsule deformation in the extensional flow in the linear regime (deformation $D_\infty \leq 0.1$), where the constant $c = 0$. For a uniform and incompressible shell material with Poisson's ratio $\nu_s = 0.5$, the Equation (11) can be rewritten as,

$$G_s = \frac{25}{6} \frac{\sigma R}{D_\infty}. \quad (12)$$

Note that the Equation (12) has the same formula with the reduced order of the prediction used in the work of Chang & Olbricht [41]. Figure 12b illustrates the linear relationship of the deformation *versus* flow stress $\sigma = \eta \dot{\epsilon}$. The capsule with a stiffer shell needs a larger flow stress to be able to be deformed. By using the Equation (12) to fit the experimental measurement, it gives the surface shear elastic modulus G_s . The bulk Young's modulus E of the shell can then be correlated by $Eh = 2G_s(1 + \nu_s) = 3G_s$.

For capsules assembled by interface complexation of chitosan and ammonium phosphatidic fatty acid (PFacid) [6, 18, 82], the Young's modulus $E \approx 6.5$ MPa. Whereas, for nylon capsules the membrane Young's modulus is around 0.1 MPa, an order of magnitude lower [41]. The surface shear modulus for chitosan capsules is invariant to the capsule size; while for HSA capsules, it is observed to increase several orders of magnitude with the capsule size (Figure 12c). The differences are due to the different kinetics of the membrane formation. In the time scale of chitosan membrane assembly (from minutes to hours), the concentrations of chitosan and the opposite-charge surfactant both are sufficient. The membrane growth of the chitosan capsules

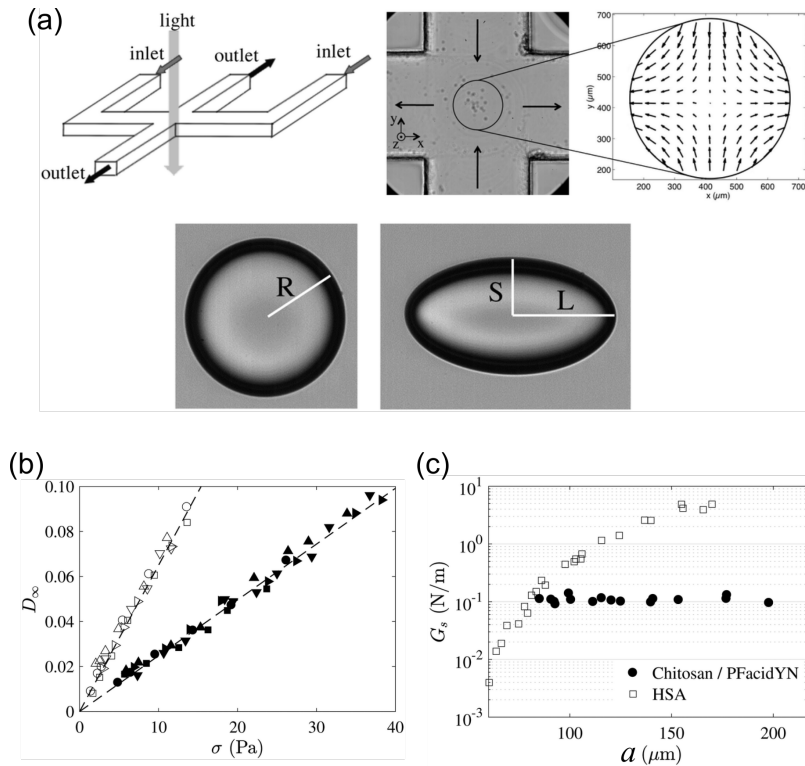


Figure 12. Microcapsule deformation in a planar extensional flow. (a) The extensional flow setup. Two opposite flow meet at the center of the chamber (stagnation point), followed by flowing away towards the two outlets. The capsule is deformed at the stagnation point. (b) The steady-state deformation D_∞ linearly increases with the hydrodynamic stress $\sigma = \eta \dot{\epsilon}$. Two batches of capsules (radius $102 \mu\text{m}$) are shown here. These two batches of capsules were prepared using different concentrations of chitosan and surfactant (ammonium phosphatidic fatty acid). The different slopes show different G_s values: 0.17 N/m for the closed symbols, and 0.065 N/m for open symbols. (c) Surface shear modulus G_s versus the capsule radius for the batch of chitosan and HSA capsules. The Young's modulus for chitosan capsules is $E \approx 6.5 \text{ MPa}$. (adapted from Ref. [6])

is predominately governed by the diffusion of the surfactant where the thickness of the capsule shell scales with time with a power of $1/2$ [6, 7, 39]. In contrast, the HSA molecules are adsorbed onto the surface and crosslinked for HSA capsules. The surface concentration of HSA increases with the capsule size. This gives rise to higher crosslinking degree in the membrane for larger size capsule, and consequently results in larger elasticity (i.e. surface shear modulus).

When the flow stress is high enough, the capsule is deformed without reaching a steady-state deformation. The capsule breaks and releases the encapsulated content [14]. The critical breakup of capsule closely depends on the surface shear modulus when this one is larger than 0.1 N/m . While, for the small value of G_s , the critical breakup stress seems to have weak dependence of the surface shear modulus (Figure 13). In breakup, the chitosan capsules [14] with high G_s exhibit an elastic-like breakage where the irregular shape is observed. Fluorescent imaging confirms that the membrane discontinuity leads to the irregular shape in the breakup process.

Compared to the shear flow, the extensional flow results in simpler capsule motion dynamics, without the observation of more complex dynamics such as tank-treading, swinging, and

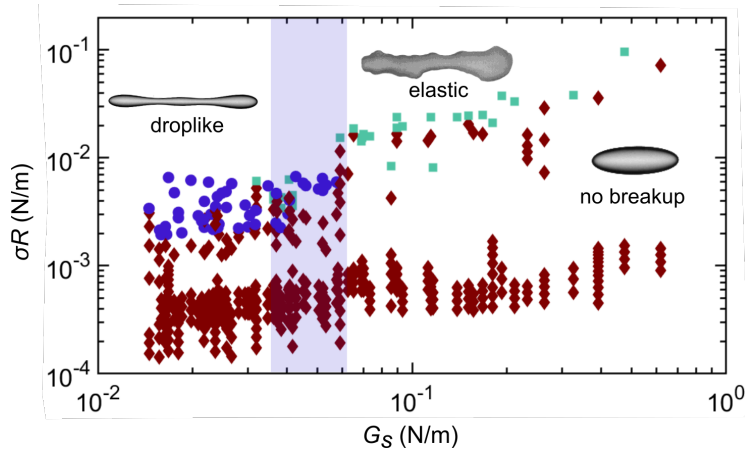


Figure 13. Phase diagram of capsule breakup in the extensional flow. The symbols \diamond , \circ and \square denote no breakup, drop-like behavior (breakup) and elastic behavior of capsules (solid-like breakup also called breakage), respectively. σ is the viscous stress, R here is the radius of capsule, and G_s is the surface shear modulus. The shaded region indicates the transition zone between drop-like and elastic behaviors breakup. Inset images are the typical shapes observed. (from Ref. [14])

tumbling [42, 96, 99]. The final deformation of the capsule in flow is stable. However, it has some limits during the experimental operation. One of the difficulties is that it requires rapid adjustment of the capsule position in flow as a small perturbation will bring the capsule away from the stagnation point. Moving out of a certain size of observation window [6, 17], the extensional rate $\dot{\epsilon}$ will significantly drop due to the walls, which should be avoided in experiments. To ensure long observation times, a computer control with fast image acquisition and processing is therefore needed, keeping the capsule near the stagnation point [100].

4.5. Characterization by non local stress: electric field

Another method avoiding the contact between a probe and a capsule membrane is to apply an external electric field to induce the membrane deformation. It is well known that vesicles [101–103] and droplets [104, 105] deform in DC and AC electric fields. A protocol has recently been proposed to measure surface viscosities in such systems by imaging the relaxation of the shape in an electric field [106]. Contrary to membranes of vesicles and polymersomes, the capsule membrane may be not electrically insulated, for example the albumin membrane. However, if the internal and external fluids have different conductivities and permittivities, it becomes possible to deform the capsules using the electric field [107–109]. This opens a new route to characterize the membrane properties as used in vesicles. A potentially high advantage of the use of an electric field is the control of the location of analysis by flow, and it is also accessible to achieve high throughput of analysis.

5. Conclusion & Outlook

The core-shell microcapsules are becoming the focus in many interdisciplinary research. The mechanical properties of microcapsules are essential not only for the fundamental studies of their dynamic behaviors in flow but also for the different purposes in applications.

In this review, we have discussed the principles of different methods for characterizing microcapsules with thin shells, i.e. with a thickness at least ten times smaller than the capsule radius. In this limit, the framework of two-dimensional elasticity can be used. In the linear regime, there are three independent parameters: the Young modulus, the Poisson's ratio, and the thickness. It is generally more convenient to use the surface shear modulus, the Poisson's ratio, and the bending modulus. Due to the difficulty in evaluating the Poisson's ratio, some authors have used the area dilation modulus K . Some shells also exhibit a viscoelastic response as observed in droplets [110], which leads to more difficult analysis by adding two additional parameters: the surface shear and dilational viscosities. On the basis of flow method and three different kinds of analysis [96, 111, 112], the shear surface viscosity has been determined with an order of magnitude which seems reasonable at the leading order. A drawback is the necessity to know the constitutive law. Unfortunately, the understanding of the nonlinear behavior (constitutive law) of shells is still a challenge even in the simplest case, i.e. purely elastic shell. Finally, two kinds of key studies would improve our understanding of the mechanics of shells. First, a cross-analysis comparing the results of the different techniques on the same capsules is still lacking. It prevents from defining their limits and their ranges of validity as in cell mechanics [113]. Second, a comparison with the mechanics of flat membranes measured by surface rheology tools should allow to decipher what is a matter of capsule (finite volume, curvature) from the general process of polymerization.

Conflicts of interest

The authors declare no competing financial interest.

Dedication

The manuscript was written through contributions of all authors. All authors have given approval to the final version of the manuscript.

Acknowledgments

M. L. thanks CNES and ANR (ANR-18-CE06-0008-01) for financial support and access to microgravity. The authors thank Zaiyi Shen and Pedro M. Resende for the careful reading of the manuscript.

References

- [1] D. Barthès-Biesel, "Motion and deformation of elastic capsules and vesicles in flow", *Annu. Rev. Fluid Mech.* **48** (2016), p. 25-52.
- [2] M. G. Bah, H. M. Bilal, J. Wang, "Fabrication and application of complex microcapsules: A review", *Soft Matter* **16** (2020), no. 3, p. 570-590.
- [3] E. Assadpour, S. M. Jafari, "Advances in spray-drying encapsulation of food bioactive ingredients: From microcapsules to nanocapsules", *Annual review of food science and technology* **10** (2019), p. 103-131.
- [4] B. Kupikowska-Stobba, D. Lewińska, "Polymer microcapsules and microbeads as cell carriers for in vivo biomedical applications", *Biomater. Sci.* **8** (2020), no. 6, p. 1536-1574.
- [5] J. Dupré de Baubigny, C. Trégouët, T. Salez, N. Pantoustier, P. Perrin, M. Reyssat, C. Monteux, "One-step fabrication of pH-responsive membranes and microcapsules through interfacial h-bond polymer complexation", *Sci. Rep.* **7** (2017), no. 1, article no. 1265.
- [6] K. Xie, C. De Loubens, F. Dubreuil, D. Z. Gunes, M. Jaeger, M. Leonetti, "Interfacial rheological properties of self-assembling biopolymer microcapsules", *Soft matter* **13** (2017), no. 36, p. 6208-6217.

- [7] R. Chachanidze, K. Xie, H. Massaad, D. Roux, M. Leonetti, C. de Loubens, "Structural characterization of the interfacial self-assembly of chitosan with oppositely charged surfactant", *Journal of Colloid and Interface Science* **616** (2022), p. 911-920.
- [8] Z. Jiang, S. Zhao, M. Yang, M. Song, J. Li, J. Zheng, "Structurally stable sustained-release microcapsules stabilized by self-assembly of pectin-chitosan-collagen in aqueous two-phase system", *Food Hydrocolloids* **125** (2022), article no. 107413.
- [9] V. Kudryavtseva, S. Boi, J. Read, R. Guillemet, J. Zhang, A. Udalov, E. Shesterikov, S. Tverdokhlebov, L. Pastorino, D. J. Gould *et al.*, "Biodegradable defined shaped printed polymer microcapsules for drug delivery", *ACS Appl. Mater. Interfaces* **13** (2021), no. 2, p. 2371-2381.
- [10] D. R. Thakare, G. Schaer, M. Yourdkhani, N. R. Sottos, "Fabrication of pH-responsive monodisperse microcapsules using interfacial tension of immiscible phases", *Soft Matter* **16** (2020), no. 22, p. 5139-5147.
- [11] M. Ina, A. P. Zhusma, N. V. Lebedeva, M. Vatankhah-Varnoosfaderani, S. D. Olson, S. S. Sheiko, "The design of wrinkled microcapsules for enhancement of release rate", *Journal of colloid and interface science* **478** (2016), p. 296-302.
- [12] Y. Xu, Y. Shen, T. C. T. Michaels, K. N. Baumann, D. Vigolo, Q. Peter, Y. Lu, K. L. Saar, D. Vella, H. Zhu *et al.*, "Deformable and Robust Core-Shell Protein Microcapsules Templated by Liquid-Liquid Phase-Separated Microdroplets", *Advanced Materials Interfaces* **8** (2021), no. 19, article no. 2101071.
- [13] B. C. Leopércio, M. Michelon, M. S. Carvalho, "Deformation and rupture of microcapsules flowing through constricted capillary", *Sci. Rep.* **11** (2021), no. 1, article no. 7707.
- [14] R. Chachanidze, K. Xie, J. Lyu, M. Jaeger, M. Leonetti, "Breakups of Chitosan microcapsules in extensional flow", *Journal of Colloid and Interface Science* **629** (2023), p. 445-454.
- [15] D. Lensen, D. M. Vriezema, J. C. M. van Hest, "Polymeric microcapsules for synthetic applications", *Macromolecular bioscience* **8** (2008), no. 11, p. 991-1005.
- [16] A. Le Goff, B. Kaoui, G. Kurzawa, B. Haszon, A.-V. Salsac, "Squeezing bio-capsules into a constriction: deformation till break-up", *Soft matter* **13** (2017), no. 41, p. 7644-7648.
- [17] C. De Loubens, J. Deschamps, M. Georgelin, A. Charrier, F. Edwards-Lévy, M. Leonetti, "Mechanical characterization of cross-linked serum albumin microcapsules", *Soft matter* **10** (2014), no. 25, p. 4561-4568.
- [18] K. Xie, "Instabilities of microcapsules in flow: breakup and wrinkles", PhD Thesis, Ecole Centrale Marseille, France, 2019.
- [19] C. Pozrikidis, *Modeling and simulation of capsules and biological cells*, Chapman & Hall/CRC Mathematical and Computational Biology, Chapman & Hall/CRC, 2003.
- [20] J. B. Freund, "Numerical simulation of flowing blood cells", *Annu. Rev. Fluid Mech.* **46** (2014), p. 67-95.
- [21] Z. Shen, A. Farutin, M. Thiébaud, C. Misbah, "Interaction and rheology of vesicle suspensions in confined shear flow", *Phys. Rev. Fluids* **2** (2017), no. 10, article no. 103101.
- [22] T. W. Secomb, "Blood flow in the microcirculation", *Annu. Rev. Fluid Mech.* **49** (2017), p. 443-461.
- [23] P. Balogh, P. Bagchi, "Direct numerical simulation of cellular-scale blood flow in 3D microvascular networks", *Biophys. J.* **113** (2017), no. 12, p. 2815-2826.
- [24] A. Viallat, M. Abkarian, *Dynamics of blood cell suspensions in microflows*, CRC Press, 2019.
- [25] M. Dionzou, A. Morere, C. Roux, B. Lonetti, J. D. Marty, C. Mingotaud, P. Joseph, D. Goudouneche, B. Payre, M. Léonetti, A. F. Mingotaud, "Comparison of methods for the fabrication and the characterization of polymer self-assemblies: what are the important parameters?", *Soft Matter* **12** (2016), p. 2166-2176.
- [26] H.-G. Döbereiner, "Properties of giant vesicles", *Current Opinion in Colloid & Interface science* **5** (2000), no. 3-4, p. 256-263.
- [27] P. M. Vlahovska, T. Podgorski, C. Misbah, "Vesicles and red blood cells in flow: From individual dynamics to rheology", *C. R. Physique* **10** (2009), no. 8, p. 775-789.
- [28] P. B. Canham, "The minimum energy of bending as a possible explanation of the biconcave shape of the human red blood cell", *J. Theor. Biol.* **26** (1970), no. 1, p. 61-81.
- [29] Z. Shen, T. M. Fischer, A. Farutin, P. M. Vlahovska, J. Harting, C. Misbah, "Blood crystal: emergent order of red blood cells under wall-confined shear flow", *Phys. Rev. Lett.* **120** (2018), no. 26, article no. 268102.
- [30] G. Boedec, M. Leonetti, M. Jaeger, "3D vesicle dynamics simulations with a linearly triangulated surface", *J. Comput. Phys.* **230** (2011), no. 4, p. 1020-1034.
- [31] W. Helfrich, "Elastic Properties of Lipid Bilayers: Theory and Possible Experiments", *Z. Naturforsch., C, J. Biosci.* **28** (1973), no. 11-12, p. 693-703.
- [32] Z. H. Huang, M. Abkarian, A. Viallat, "Sedimentation of vesicles: from pear-like shapes to microtether extrusion", *New J. Phys.* **13** (2011), no. 3, article no. 035026.
- [33] G. Boedec, M. Jaeger, M. Leonetti, "Sedimentation-induced tether on a settling vesicle", *Phys. Rev. E* **88** (2013), no. 1, article no. 010702.
- [34] E. A. Evans, "Bending resistance and chemically induced moments in membrane bilayers", *Biophys. J.* **14** (1974), no. 12, p. 923-931.

- [35] G. Boedec, M. Jaeger, M. Leonetti, "Settling of a vesicle in the limit of quasispherical shapes", *J. Fluid Mech.* **690** (2012), p. 227-261.
- [36] G. Couplier, A. Farutin, C. Minetti, T. Podgorski, C. Misbah, "Shape diagram of vesicles in Poiseuille flow", *Phys. Rev. Lett.* **108** (2012), no. 17, article no. 178106.
- [37] S. Knoche, D. Vella, E. Aumaitre, P. Degen, H. Rehage, P. Cicuti, J. Kierfeld, "Elastometry of deflated capsules: Elastic moduli from shape and wrinkle analysis", *Langmuir* **29** (2013), no. 40, p. 12463-12471.
- [38] M.-C. Andry, F. Edwards-Lévy, M.-C. Lévy, "Free amino group content of serum albumin microcapsules. III. A study at low pH values", *International journal of pharmaceuticals* **128** (1996), no. 1-2, p. 197-202.
- [39] D. Z. Gunes, M. Pouzot, M. Rouvet, S. Ulrich, R. Mezzenga, "Tuneable thickness barriers for composite o/w and w/o capsules, films, and their decoration with particles", *Soft Matter* **7** (2011), no. 19, p. 9206-9215.
- [40] J. Dupré de Baubigny, P. Perrin, N. Pantoustier, T. Salez, M. Reyssat, C. Monteux, "Growth mechanism of polymer membranes obtained by H-bonding across immiscible liquid interfaces", *ACS Macro Lett.* **10** (2021), no. 2, p. 204-209.
- [41] K.-S. Chang, W. L. Olbricht, "Experimental studies of the deformation of a synthetic capsule in extensional flow", *J. Fluid Mech.* **250** (1993), p. 587-608.
- [42] I. Koleva, H. Rehage, "Deformation and orientation dynamics of polysiloxane microcapsules in linear shear flow", *Soft Matter* **8** (2012), no. 13, p. 3681-3693.
- [43] C. De Loubens, J. Deschamps, G. Boedec, M. Leonetti, "Stretching of capsules in an elongation flow, a route to constitutive law", *J. Fluid Mech.* **767** (2015).
- [44] E. Lac, D. Barthès-Biesel, N. A. Pelekasis, J. Tsamopoulos, "Spherical capsules in three-dimensional unbounded Stokes flows: effect of the membrane constitutive law and onset of buckling", *J. Fluid Mech.* **516** (2004), p. 303-334.
- [45] D. Barthès-Biesel, "Capsule motion in flow: Deformation and membrane buckling", *C. R. Physique* **10** (2009), no. 8, p. 764-774.
- [46] D. Barthès-Biesel, A. Diaz, E. Dhenin, "Effect of constitutive laws for two-dimensional membranes on flow-induced capsule deformation", *J. Fluid Mech.* **460** (2002), p. 211-222.
- [47] R. Skalak, A. Tozeren, R. P. Zarda, S. Chien, "Strain energy function of red blood cell membranes", *Biophys. J.* **13** (1973), no. 3, p. 245-264.
- [48] S. Knoche, J. Kierfeld, "Buckling of spherical capsules", *Phys. Rev. E* **84** (2011), no. 4, article no. 046608.
- [49] A. Ghaemi, A. Philipp, A. Bauer, K. Last, A. Fery, S. Gekle, "Mechanical behaviour of micro-capsules and their rupture under compression", *Chemical Engineering Science* **142** (2016), p. 236-243.
- [50] F. Risso, M. Carin, "Compression of a capsule: Mechanical laws of membranes with negligible bending stiffness", *Phys. Rev. E* **69** (2004), no. 6, article no. 061601.
- [51] K. S. Cole, "Surface forces of the Arbacia egg", *Journal of Cellular and Comparative Physiology* **1** (1932), no. 1, p. 1-9.
- [52] A. Rehor, L. Canaple, Z. Zhang, D. Hunkeler, "The compressive deformation of multicomponent microcapsules: Influence of size, membrane thickness, and compression speed", *Journal of Biomaterials Science, Polymer Edition* **12** (2001), no. 2, p. 157-170.
- [53] M. Carin, D. Barthès-Biesel, F. Edwards-Lévy, C. Postel, D. C. Andrei, "Compression of biocompatible liquid-filled HSA-alginate capsules: Determination of the membrane mechanical properties", *Biotechnology and bioengineering* **82** (2003), no. 2, p. 207-212.
- [54] E. Häner, M. Heil, A. Juel, "Deformation and sorting of capsules in a T-junction", *J. Fluid Mech.* **885** (2020).
- [55] E. Reissner, "Stresses and small displacements of shallow spherical shells. I", *Journal of Mathematics and Physics* **25** (1946), no. 1-4, p. 80-85.
- [56] A. Lytra, V. Sboros, A. Giannakopoulos, N. A. Pelekasis, "Modeling atomic force microscopy and shell mechanical properties estimation of coated microbubbles", *Soft Matter* **16** (2020), no. 19, p. 4661-4681.
- [57] Y.-H. Huang, F. Salmon, A. Kamble, A. X. Xu, M. Michelin, B. C. Leópolis, M. S. Carvalho, J. M. Frostad, "Models for the mechanical characterization of core-shell microcapsules under uniaxial deformation", *Food Hydrocolloids* **119** (2021), article no. 106762.
- [58] W. W. Feng, W.-H. Yang, "On the Contact Problem of an Inflated Spherical Nonlinear Membrane", *J. Appl. Mech.* **40** (1973), no. 1, p. 209-214.
- [59] M. P. Neubauer, M. Poehlmann, A. Fery, "Microcapsule mechanics: From stability to function", *Advances in colloid and interface science* **207** (2014), p. 65-80.
- [60] K. Xie, A. Glasser, S. Shinde, Z. Zhang, J.-M. Rampoux, A. Maali, E. Cloutet, G. Hadziioannou, H. Kellay, "Delamination and wrinkling of flexible conductive polymer thin films", *Advanced Functional Materials* **31** (2021), no. 21, article no. 2009039.
- [61] Z. Zhang, V. Bertin, M. Arshad, E. Raphael, T. Salez, A. Maali, "Direct measurement of the elastohydrodynamic lift force at the nanoscale", *Phys. Rev. Lett.* **124** (2020), no. 5, article no. 054502.
- [62] F. Dubreuil, N. Elsner, A. Fery, "Elastic properties of polyelectrolyte capsules studied by atomic-force microscopy and RICM", *Eur. Phys. J. E* **12** (2003), no. 2, p. 215-221.
- [63] T. X. Chu, A.-V. Salsac, E. Leclerc, D. Barthès-Biesel, H. Wurtz, F. Edwards-Lévy, "Comparison between measure-

- ments of elasticity and free amino group content of ovalbumin microcapsule membranes: discrimination of the cross-linking degree”, *Journal of colloid and interface science* **355** (2011), no. 1, p. 81-88.
- [64] J. Cappello, V. d’Herbement, A. Lindner, O. Du Roure, “Microfluidic in-situ measurement of Poisson’s ratio of hydrogels”, *Micromachines* **11** (2020), no. 3, p. 318.
- [65] Y. Li, Z. Hu, C. Li, “New method for measuring Poisson’s ratio in polymer gels”, *Journal of applied polymer science* **50** (1993), no. 6, p. 1107-1111.
- [66] M. Pretzl, M. P. Neubauer, M. Tekaath, C. Kunert, C. Kuttner, G. Leon, D. Berthier, P. Erni, L. Ouali, A. Fery, “Formation and mechanical characterization of aminoplast core/shell microcapsules”, *ACS Appl. Mater. Interfaces* **4** (2012), no. 6, p. 2940-2948.
- [67] M. D. Biviano, L. J. Böni, J. D. Berry, P. Fischer, R. R. Dagastine, “Viscoelastic characterization of the crosslinking of β -lactoglobulin on emulsion drops via microcapsule compression and interfacial dilational and shear rheology”, *Journal of colloid and interface science* **583** (2021), p. 404-413.
- [68] K. L. Johnson, K. Kendall, A. D. Roberts, “Surface energy and the contact of elastic solids”, *Proceedings of the royal society of London. A. mathematical and physical sciences* **324** (1971), no. 1558, p. 301-313.
- [69] A. Aniskevich, V. Kulakov, O. Bulderberga, P. Knotek, J. Tedim, F. Maia, V. Leisis, D. Zeleniakienė, “Experimental characterisation and modelling of mechanical behaviour of microcapsules”, *Journal of Materials Science* **55** (2020), no. 27, p. 13457-13471.
- [70] G. R. Plaza, T. Q. P. Uyeda, Z. Mirzaei, C. A. Simmons, “Study of the influence of actin-binding proteins using linear analyses of cell deformability”, *Soft Matter* **11** (2015), no. 27, p. 5435-5446.
- [71] B. González-Bermúdez, G. V. Guinea, G. R. Plaza, “Advances in micropipette aspiration: applications in cell biomechanics, models, and extended studies”, *Biophys. J.* **116** (2019), no. 4, p. 587-594.
- [72] E. H. Zhou, C. T. Lim, S. T. Quek, “Finite element simulation of the micropipette aspiration of a living cell undergoing large viscoelastic deformation”, *Mech. Adv. Mater. Struct.* **12** (2005), no. 6, p. 501-512.
- [73] D. P. Theret, M. J. Levesque, M. Sato, R. M. Nerem, L. T. Wheeler, “The Application of a Homogeneous Half-Space Model in the Analysis of Endothelial Cell Micropipette Measurements”, *J. Biomech. Eng.* **110** (1988), no. 3, p. 190-199.
- [74] J. R. Henriksen, J. H. Ipsen, “Measurement of membrane elasticity by micro-pipette aspiration”, *Eur. Phys. J. E* **14** (2004), no. 2, p. 149-167.
- [75] J. Hegemann, S. Knoche, S. Egger, M. Kott, S. Demand, A. Unverfehrt, H. Rehage, J. Kierfeld, “Pendant capsule elastometry”, *Journal of colloid and interface science* **513** (2018), p. 549-565.
- [76] J. Walter, A.-V. Salsac, D. Barthès-Biesel, P. Le Tallec, “Coupling of finite element and boundary integral methods for a capsule in a Stokes flow”, *Int. J. Numer. Methods Eng.* **83** (2010), no. 7, p. 829-850.
- [77] G. Boedec, M. Leonetti, M. Jaeger, “Isogeometric FEM-BEM simulations of drop, capsule and vesicle dynamics in Stokes flow”, *J. Comput. Phys.* **342** (2017), p. 117-138.
- [78] Y. Sui, Y.-T. Chew, P. Roy, H.-T. Low, “A hybrid method to study flow-induced deformation of three-dimensional capsules”, *J. Comput. Phys.* **227** (2008), no. 12, p. 6351-6371.
- [79] S. B. Q. Tran, Q. T. Le, F. Y. Leong, D. V. Le, “Modeling deformable capsules in viscous flow using immersed boundary method”, *Phys. Fluids* **32** (2020), no. 9, article no. 093602.
- [80] J. Ma, L. Xu, F.-B. Tian, J. Young, J. C. S. Lai, “Dynamic characteristics of a deformable capsule in a simple shear flow”, *Phys. Rev. E* **99** (2019), no. 2, article no. 023101.
- [81] W. R. Dodson, P. Dimitrakopoulos, “Dynamics of strain-hardening and strain-softening capsules in strong planar extensional flows via an interfacial spectral boundary element algorithm for elastic membranes”, *J. Fluid Mech.* **641** (2009), p. 263-296.
- [82] M. Maleki, C. de Loubens, K. Xie, E. Talansier, H. Bodiguel, M. Leonetti, “Membrane emulsification for the production of suspensions of uniform microcapsules with tunable mechanical properties”, *Chemical Engineering Science* **237** (2021), article no. 116567.
- [83] G. Kaufman, R. Boltyskiy, S. Nejati, A. R. Thiam, M. Loewenberg, E. R. Dufresne, C. O. Osuji, “Single-step microfluidic fabrication of soft monodisperse polyelectrolyte microcapsules by interfacial complexation”, *Lab on a Chip* **14** (2014), no. 18, p. 3494-3497.
- [84] C. Tregouët, T. Salez, C. Monteux, M. Reyssat, “Microfluidic probing of the complex interfacial rheology of multilayer capsules”, *Soft matter* **15** (2019), no. 13, p. 2782-2790.
- [85] D. Barthès-Biesel, J.-M. Rallison, “The time-dependent deformation of a capsule freely suspended in a linear shear flow”, *J. Fluid Mech.* **113** (1981), p. 251-267.
- [86] D. Barthès-Biesel, H. Sgaier, “Role of membrane viscosity in the orientation and deformation of a spherical capsule suspended in shear flow”, *J. Fluid Mech.* **160** (1985), p. 119-135.
- [87] C. Pozrikidis *et al.*, *Boundary integral and singularity methods for linearized viscous flow*, Cambridge Texts in Applied Mathematics, Cambridge University Press, 1992.
- [88] J. Gubspun, C. de Loubens, R. Trozzo, J. Deschamps, M. Georgelin, F. Edwards-Lévy, M. Leonetti, “Perturbations of the flow induced by a microcapsule in a capillary tube”, *Fluid Dynamics Research* **49** (2017), no. 3, article no. 035501.

- [89] J. Gubspun, P.-Y. Gires, C. de Loubens, D. Barthès-Biesel, J. Deschamps, M. Georgelin, M. Leonetti, E. Leclerc, F. Edwards-Lévy, A.-V. Salsac, "Characterization of the mechanical properties of cross-linked serum albumin microcapsules: effect of size and protein concentration", *Colloid. Polym. Sci.* **294** (2016), no. 8, p. 1381-1389.
- [90] F. Risso, F. Collé-Paillot, M. Zagzoule, "Experimental investigation of a bioartificial capsule flowing in a narrow tube", *J. Fluid Mech.* **547** (2006), p. 149-173.
- [91] X.-Y. Wang, A. Merlo, C. Dupont, A.-V. Salsac, D. Barthès-Biesel, "A microfluidic methodology to identify the mechanical properties of capsules: comparison with a microrheometric approach", *Flow* **1** (2021).
- [92] C. Quesada, C. Dupont, P. Villon, A.-V. Salsac, "Diffuse approximation for identification of the mechanical properties of microcapsules", *Mathematics and Mechanics of Solids* **26** (2021), no. 7, p. 1018-1028.
- [93] A. Walter, H. Rehage, H. Leonhard, "Shear-induced deformations of polyamide microcapsules", *Colloid. Polym. Sci.* **278** (2000), no. 2, p. 169-175.
- [94] H. Rehage, M. Husmann, A. Walter, "From two-dimensional model networks to microcapsules", *Rheologica acta* **41** (2002), no. 4, p. 292-306.
- [95] S. Joung, M. Song, D. Kim, "Synthetic capsule breakup in simple shear flow", *Phys. Fluids* **32** (2020), no. 11, article no. 113603.
- [96] C. De Loubens, J. Deschamps, F. Edwards-Lévy, M. Leonetti, "Tank-treading of microcapsules in shear flow", *J. Fluid Mech.* **789** (2016), p. 750-767.
- [97] G. I. Taylor, "The formation of emulsions in definable fields of flow", *Proc. R. Soc. Lond. A* **146** (1934), no. 858, p. 501-523.
- [98] J. Deschamps, V. Kantsler, E. Segre, V. Steinberg, "Dynamics of a vesicle in general flow", *Proc. Natl. Acad. Sci. USA* **106** (2009), no. 28, p. 11444-11447.
- [99] H. Noguchi, "Swinging and synchronized rotations of red blood cells in simple shear flow", *Phys. Rev. E* **80** (2009), no. 2, article no. 021902.
- [100] M. Vona, E. Lauga, "Stabilizing viscous extensional flows using reinforcement learning", *Phys. Rev. E* **104** (2021), no. 5, article no. 055108.
- [101] M. Kummrow, W. Helfrich, "Deformation of giant lipid vesicles by electric fields", *Phys. Rev. A* **44** (1991), no. 12, p. 8356-8360.
- [102] R. Dimova, K. A. Riske, S. Aranda, N. Bezlyepkina, R. L. Knorr, R. Lipowsky, "Giant vesicles in electric fields", *Soft matter* **3** (2007), no. 7, p. 817-827.
- [103] R. Dimova, N. Bezlyepkina, M. D. Jordö, R. L. Knorr, K. A. Riske, M. Staykova, P. M. Vlahovska, T. Yamamoto, P. Yang, R. Lipowsky, "Vesicles in electric fields: Some novel aspects of membrane behavior", *Soft Matter* **5** (2009), no. 17, p. 3201-3212.
- [104] O. Vizika, D. A. Saville, "The electrohydrodynamic deformation of drops suspended in liquids in steady and oscillatory electric fields", *J. Fluid Mech.* **239** (1992), p. 1-21.
- [105] J. R. Melcher, G. I. Taylor, "Electrohydrodynamics: a review of the role of interfacial shear stresses", *Annu. Rev. Fluid Mech.* **1** (1969), no. 1, p. 111-146.
- [106] H. A. Faizi, R. Dimova, P. M. Vlahovska, "A vesicle microrheometer for high-throughput viscosity measurements of lipid and polymer membranes", *Biophys. J.* **121** (2022), no. 6, p. 910-918.
- [107] R. B. Karyappa, S. D. Deshmukh, R. M. Thaokar, "Deformation of an elastic capsule in a uniform electric field", *Phys. Fluids* **26** (2014), no. 12, article no. 122108.
- [108] S. Puri, R. M. Thaokar, "Study of dependence of elasticity on the microstructure of microcapsules using electrodeformation technique", *Colloids and Surfaces A: Physicochemical and Engineering Aspects* **569** (2019), p. 179-189.
- [109] S. Das, R. M. Thaokar, "Large-deformation electrohydrodynamics of an elastic capsule in a DC electric field", *J. Fluid Mech.* **841** (2018), p. 489-520.
- [110] J. Gounley, G. Boedec, M. Jaeger, M. Leonetti, "Influence of surface viscosity on droplets in shear flow", *J. Fluid Mech.* **791** (2016), p. 464-494.
- [111] T. Lin, Z. Wang, R. Lu, W. Wang, Y. Sui, "A high-throughput method to characterize membrane viscosity of flowing microcapsules", *Phys. Fluids* **33** (2021), no. 1, article no. 011906.
- [112] T. Lin, Z. Wang, W. Wang, Y. Sui, "A neural network-based algorithm for high-throughput characterisation of viscoelastic properties of flowing microcapsules", *Soft Matter* **17** (2021), no. 15, p. 4027-4039.
- [113] P.-H. Wu, D. R.-B. Aroush, A. Asnacios, W.-C. Chen, M. E. Dokukin, B. L. Doss, P. Durand, A. Ekpenyong, J. Guck, N. V. Guz *et al.*, "Comparative study of cell mechanics methods", *Nature methods* **15** (2018), no. 7, p. 491-498.